Supplementary information

S1 Stability of peptide-modified GNPs within a cell culture medium

We incubated our peptide-conjugated NPs in a cell culture medium overnight and measured their stability using Dynamic Light Scattering (DLS) and UV visible spectroscopy.

Table S1. Measuring the stability of peptide-modified GNPs using DLS and UV.

	Citrate-capped NPs in PBS	Peptide-capped NPs in PBS	Citrate-capped NPs in cell culture media	Peptide-capped NPs in cell culture media
UV (peak wavelength- nm)	519	523	527	523
DLS-hydrodynamic diameter (nm)	18.2±0.1	20.5±0.2	23.5±0.2	21.0±0.3

As shown in Table S1, DLS and UV data showed that the size of the peptide-modified GNPs remains unaffected in the tissue culture media while the size of the citrate-capped GNPs changed due to the attachment of serum proteins.[1]

S2. Evaluation of cytotoxicity due to peptide-modified GNPs

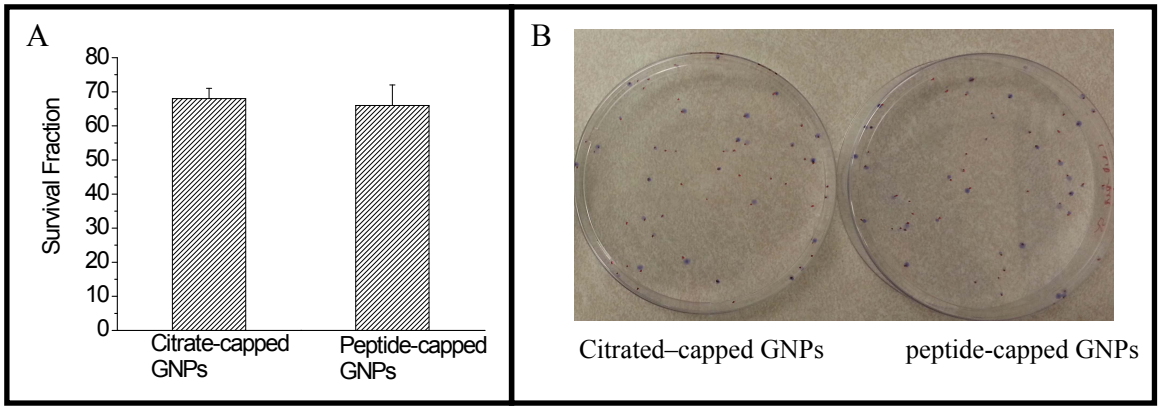

Figure S2. Cytotoxicity due to peptide-modified GNPs. A. Survival fraction generated from a Clonogenic assay. B. Colonies formed on tissue culture dishes.

The cytotoxicity due to peptide-modified GNPs was compared to citrate-capped GNPs using a clonogenic assay.[2] This assay can be used to measure the long term toxicity effects. In short term, we measured the cytotoxicity using trypan blue exclusion assay. There was no short-term or long-term cytotoxicity introduced by peptide modified NPs.

HeLa cells were grown in DMEM/h21 medium at 37°C in a humidified incubator with 95% air/5% CO_2. The cells were first seeded at 10^6 cells in four tissue culture dishes and were incubated for 24 hours. The cells were then incubated with GNPs overnight. Following the incubation, the cells were trypsinized , counted, and plated in 10 cm tissue culture dishes. We plated 100 cells per dish. Cells were incubated for 2 weeks to form colonies. Methylene blue (0.1%) was used for staining the colonies. The colonies containing >50 cells were counted for calculating the surviving fractions. The plating efficiency of the cells was determined by taking the ratio of the number of colonies formed to the number of cells seeded. This is done using reference cells where no GNPs were introduced into the tissue culture medium. The survival fraction of cells once incubated with GNPs was calculated as follows:

Survival fraction = (colonies formed/ (cells seeded x plating efficiency)

Figure S2.A shows that there was no significant difference in the cell survival for cells incubated with peptide-modified GNPs in comparison to citrate-capped GNPs. The Figure S2.B shows the two petri dishes stained with methylene blue to visualize the colonies. The blue dots are colonies.

S3 CytoViva imaging

1. Differentiating aggregated vs. non-aggregated NPs using CytoViva technology

The images below show the system's ability to distinguish aggregated from mono-dispersed GNPs. Two sample slides were prepared: one with GNPs aggregated *via* media and another with a non-aggregated set from the same GNP sample. The spectral angle mapper was employed to map the images with the sample spectra shown. On the right, the SAM map is displayed using a threshold spectral angle of 0.1 radians. The spectra from the aggregated sample (left panel) show a distinct red shift that is clearly visible in

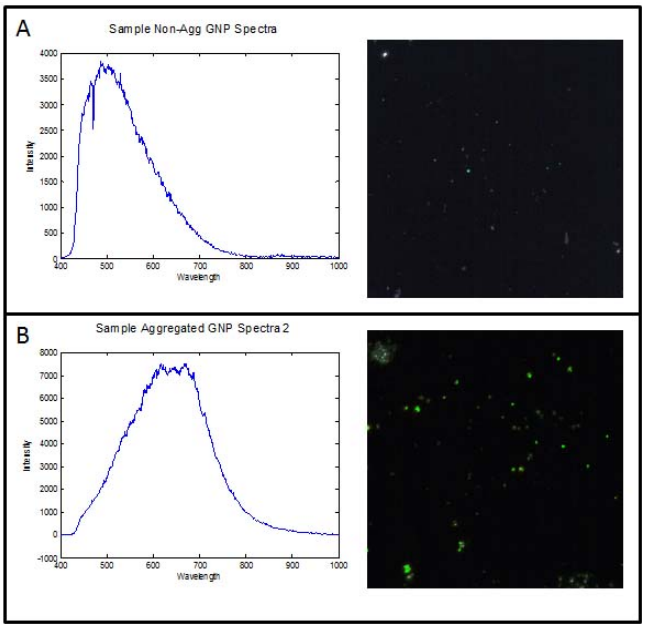

Figure S3.1. Hypersepctral imaging of monodispersed and aggregated GNPs. A-B. Reflectance spectra (left) and mapped images based on the reflectance spectra on the left monodispersed and aggregated GNPs, respectively.

2. CytoViva Analysis of Cells with Internalized Nanoparticles

This CytoViva technology was specifically designed for optical observation and spectral confirmation of NPs as they interact with cells and tissues. The illumination of the microscope system utilizes oblique angle lighting to create high signal-to-noise optimized dark-field based images. **Figure S3.2A** is a dark-field image of a group of cells with internalized GNPs. The GNPs appear bright owing to their high scattering cross-section. With the integrated CytoViva hyperspectral imaging capability, reflectance spectra from specific materials can be captured and measured. The SAM (Spectral Angle Mapping) is an automated procedure used to determine whether GNPs are present in the input image, and locates which pixels contain the material of interest. SAM accomplishes these tasks by comparing unknown spectra in hyperspectral imagery with known spectra for the material of interest (GNPs in this case). The hyperspectral image displays the relative degree to which unknown spectra in each image pixel match the known GNP spectrum. **Figure S3.2B** shows the hyperspectral image with an overlaid spectral angle map where the red dots represent GNPs. **Figure S3.2C** illustrates the reflectance spectra from one of the red dots while the spectrum (white in colour) shows that it is quite similar

to the reflectance spectrum of GNPs[3, 4]. It can be clearly seen that the GNP clusters have a very high reflection compared to the background.

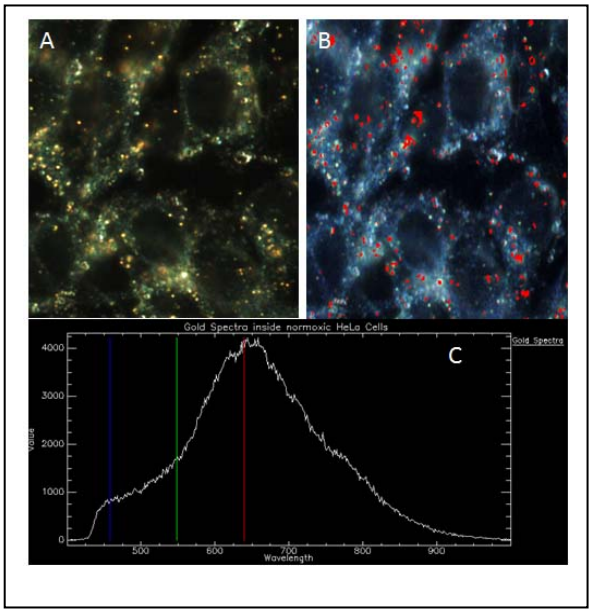

Figure S3.2. CytoViva Hyperspectral imaging of GNPs internalized in cells. A) The dark-field image of GNPs in cells. B) The spectral angle map overlaid onto the hyperspectral dark-field image. The spectrum from each pixel is compared with a reflectance spectra from gold and if a match is determined, the pixels are coloured red. C) The reflectance spectra from one of the gold clusters (white solid line) and the background reflectance from the nucleus (red solid line) and the cytoplasm (green solid line).The spectra from each pixel in Figure 3B is compared with this spectra and if a match is determined, the pixels are coloured red.

3. Three dimensional imaging (3D imaging)

Shown below is an example of a few of the 322 2D slices that were used to create the 3D volumetric images. The original slices were separated by 400 nm before being collapsed *via* interpolation to produce smoother 3D images. The spatial resolution of the image pixels in the XY direction are 64.5nm. This is calculated by taking the camera pixel size at 1x, which is 6450nm, and dividing it by the magnification which was 100x for these image stacks. The Z resolution was set to 400nm, thus 1 pixel is 64.5nm x 64.5nm x 400nm thick. The software then interpolated a pixel to create more Z slices to form each pixel square.

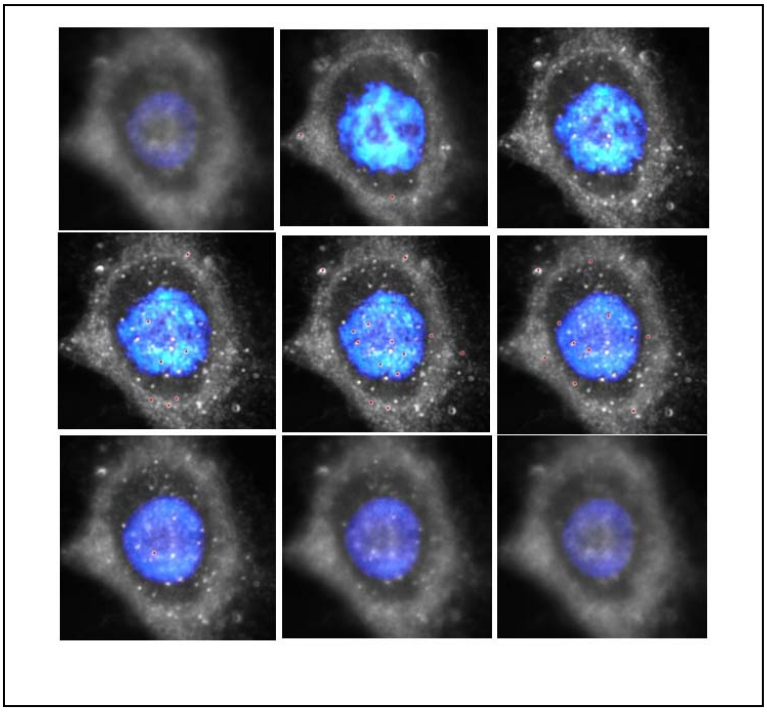

Figure S3.3. Few 2D slices from 3D images to show how GNPs located.

GNPs were matched using spectra angle mapping and appear as red dots in the image. The GNPs were matched within a spectral angle threshold of 0.1 radians using the Spectral Angle Mapper (SAM). As the scanner proceeds through the sample, a given GNP's reflectance intensity increases or decreases relative to the GNP's distance from the current plane. When the GNP intensity is at the highest level, the software labels it with a red pixel as shown above. This feature can thus be used to qualitatively detect GNPs at various depths in the sample.

The analysis of the individual slices that make-up the 3D images allow for rough qualitative counts of GNPs both inside and outside the nucleus. For example, in the images above, the nucleus is clearly labelled in blue, and GNPs that have reached their highest intensity in the current plane are labeled as red dots. By detecting red pixels in each slice, the overall number of GNPs in any given plane can be counted. By calculating the total sum of these over all the slices, the total number of GNPs in the sample can be determined. Furthermore, by searching within a 6x6 pixel square around any detected GNPs for blue

pixels (labelled nucleus), the number of GNPs in the nucleus can also be detected and summed over all the slices. This analysis was done *via* the program *Matlab*, and the results are tabulated below showing a rough count of GNPs both inside and outside the nucleus.

Figure 7 in the manuscript displays a 3D construction of GNPs localized within a cell targeted with peptide-capped GNPs. Based on that image; we were able to calculate the percentage of NPs within the nucleus as illustrated in the table below.

	Total in Sample	**Inside Nucleus**	**Percentage of GNPs in Nucleus**
No. of GNPs	56	20	35.71%

S4 Details of Exocytosis of peptide-capped GNPs.

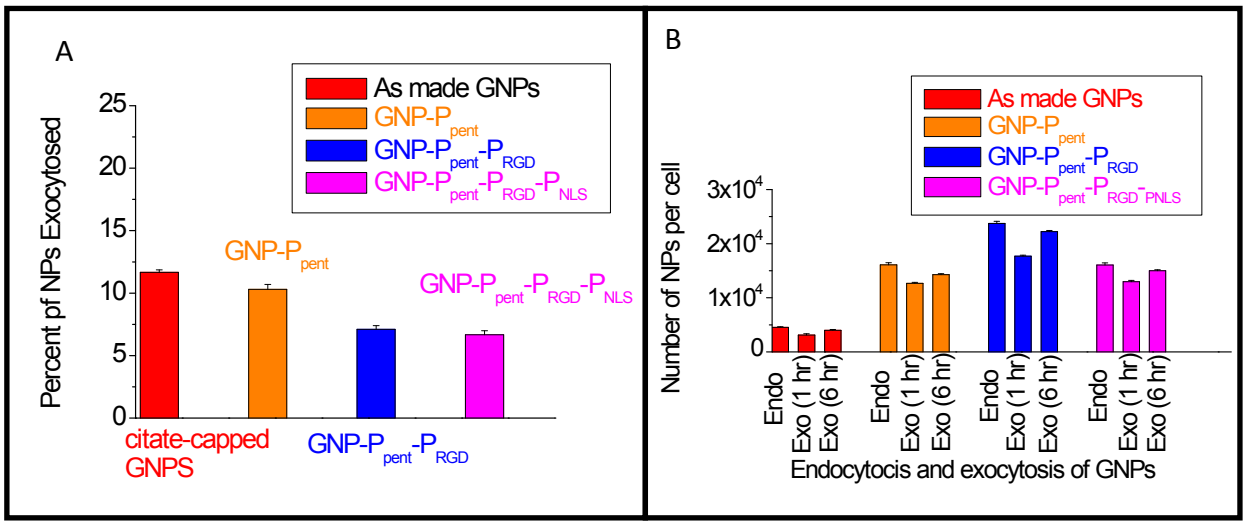

Figure S4. Exocytosis of peptide-capped GNPs. A, Percent of NPs exocytosed for cells incubated with citrate-capped, pentapeptide-capped, RGD peptide in combination with pentapeptide, and RGD, NLS, and pentapeptide modified GNPs. B, Dynamics of exocytosis process following one and six hours.

Citrate-capped and pentapeptide-capped GNPs were localized within endosomes, followed by their processing *via* fusion with lysosomes as discussed in previous studies.[5, 6] NPs localized in lysosomes were excreted into the extracellular matrix by fusing with the cell membrane. Once the GNPs were capped with RGD peptide in addition to the pentapeptide, some of the GNPs were able to enter the cytoplasm. When the GNPs were capped with NLS

peptide in combination with RGD peptide, several of the GNPs localized in the cytoplasm were able to enter the nucleus. Previous studies have shown that the NPs localized in either the nucleus or cytoplasm, have a slower excretion capability as compared to NPs localized in lysosomes. For example, Wang *et al*. evaluated the excretion of CuO NPs in A549 cells and discovered that a portion of NPs, which were located in mitochondria and nucleus, could not be excreted by the cells.[7] Similarly, based on findings by Chu *et al*., clusters of silica NPs in lysosomes were more easily exocytosed by H1299 cells as compared to single NPs in the cytoplasm.[8]

References

1 B. D. Chithrani and W. C. W. Chan, *Nano Lett.*, 2007, **7**, 1542-1550.

2 B. D. Chithrani, S. Jelveh, F. Jalali, M. Van Prooijen, C. Allen, R. G. Bristow, R. P. Hill and D. A. Jaffray, *Radiat. Res.*, 2010, **173**, 719–728.

3 J. C. Y. Kah, K. W. Kho, C. G. L. Lee, C. J. R. Sheppard, Z. X. Shen, K. C. Soo and M. C. Olivo, *Int. J. Namomed.*, 2007, **2**, 785-798.

4 J. A. Viator, S. Gupta, B. S. Goldschmidt, K. Bhattacharyyal, R. Kannan, R. Shukla, P. S. Dale, E. Boote and K. Katti, *J. Biomed. Nanotechnol.*., 2010, **6**, 187-191.

5 P. Nativo, I. A. Prior, and M. Brust, *ACS Nano*, 2008, **2**, 1639-1644.

6 B. D. Chithrani, A. A. Ghazani and W. C. W. Chan, *Nano Lett.*, 2006, **6**, 662-668.

7 Z. Wang, N. Li, J. Zhao, J. C. White, P. Qu and B. Xing, *Chem. Res. Toxicol.,* 2012, **25**, 1512–1521.

8 Z. Chu, Y. Huang, Q. Tao, and Q. Li, *Nanoscale*, 2011, **3**, 3291–3299.